# CHAPTER-1

# INTRODUCTION

## 1.1 Introduction

The theory of Isostasy refers to the state of gravitational equilibrium between the earth's lithosphere and asthenosphere, and assumes that the tectonic plates float at an elevation depending upon their thickness and density. The term Isostasy is derived from the Greek words "ísos" and "stásis" meaning equal standing. The concept of Isostasy was introduced in order to explain how different topographic loads can exist at the Earth's surface. Several models exist to explain the theory of Isostasy which is classified as Local Isostasy (Airy and Pratt model) and Regional Isostasy (Vening Meinesz model).

In order to explain the anomalous plumb line deflection near mountain belts like the Himalayas and the Andes, G. B. Airy in 1855 suggested that the excess load of the topographic rises is compensated by the buoyancy force acting on the surface of equilibrium. In Airy's model (Figure 1.1a) the crustal density is constant and Isostatic compensation is achieved by a variation in the crustal thickness. Four years later, in 1859, J. H. Pratt brought forward a different explanation suggesting that the excess load of the mountains is compensated by lateral density variations within the crust (Figure 1.1b). The hypotheses that they have in common is that, the compensation of the extra mass of a mountain above sea level is obtained locally by a less dense region (root) below sea level, but their explanations differ in the way it was achieved.

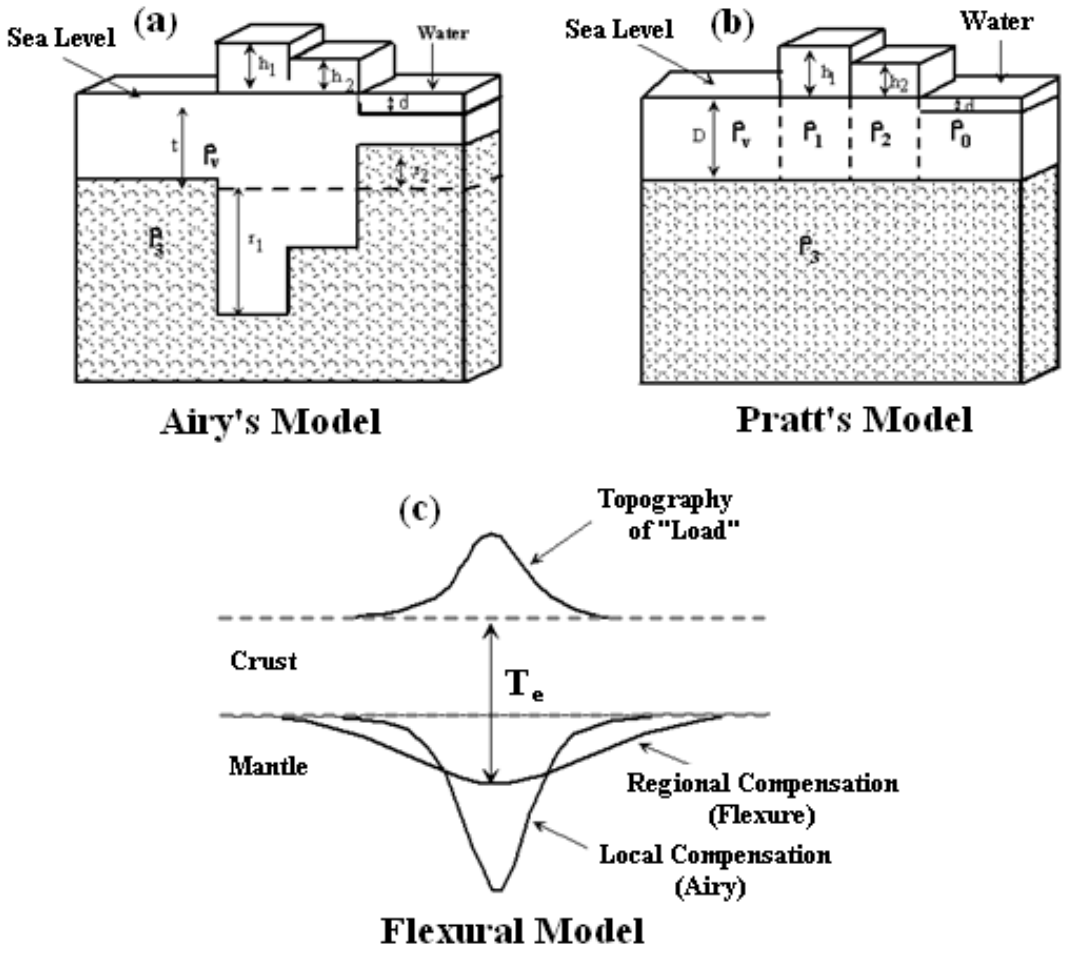


**Figure 1.1:** Isostatic Models and Methods of Compensation: (a) Airy's Model, (b) Pratt's Model, (c) Flexural Model.

The Flexural Isostasy model, more commonly referred to as the Regional Isostasy model (Figure 1.1c), is based on the Vening Meinesz model. The Flexural Isostasy model assumes that the continental or oceanic lithosphere is a thin elastic plate overlying an inviscid fluid (Watts, 2001) that flexes elastically in response to external and internal loads. External load refers to the topographic load and internal load is crustal inhomogeneities within the plate due to lateral density variations. Compensation is achieved on a geological scale by the deflection of the elastic lithospheric plate due to surface and subsurface loads. The Regional model of Vening Meinesz is similar to the

Airy model. In addition to the buoyancy force due to density contrast between the crust and mantle, the flexural rigidity (D) of the bent lithospheric plate is considered.

Flexural rigidity 'D' is a measure of the strength of the thin elastic lithospheric plate given by,

$$D = \frac{ET_e^3}{12(1-\sigma^2)} \quad (1.1)$$

where E is the Young's modulus, $T_e$ is the elastic thickness and $\sigma$ is the Poisson's ratio.

### 1.2 Effective Elastic Thickness ($T_e$)

The effective elastic thickness of the lithosphere is defined as the thickness of an equivalent elastic plate which would produce the same deflection under the known tectonic loading structure. Since the lithosphere is composed of several layers, which may fail inelastically in both brittle and ductile fashion, $T_e$ represents the integral strength of the lithosphere within limits imposed by the rheology of the lithosphere (Burov and Diament, 1995). The elastic thickness depends on a number of geophysical properties such as the stresses acting on the lithospheric plate, its thermal state, composition, geometry, crustal thickness, etc. (Burov and Diament, 1995; Lowry and Smith, 1995; Lowry et al., 2000). Hence, $T_e$ can be used as a proxy to map variation in lithospheric rheology; its spatial variation can reflect the lateral variation of lithospheric properties.

The loads on the lithosphere are supported by a quasi-elastic layer (Goetze and Evans, 1979) that is capable of supporting loads for long periods (i.e., > $10^5$ yr). This elastic core that separates the brittle and ductile deformation fields later became popular measure to define $T_e$ (Burov and Diament, 1995). A compilation of 139 published $T_e$ estimates (Watts, 2001) in oceanic regions suggests that there is a good correlation

between the flexural rigidity and the age of the lithosphere at the time of loading. The elastic thickness in oceanic regions has values between 0 and 65 km (Watts, 1978). However, in case of continental areas no such correlation is found. The existing 82 estimates of $T_e$ in continental areas are scattered within the values 0 to130 km and has no simple dependency on load age (Watts, 2001). The responses of the continental and oceanic lithospheres to long-term loads differ as a result of their distinct physical and chemical evolution. The composition and thermal regime of the continental lithosphere are more complicated than for the oceans and there has been much debate on the meaning of $T_e$ for the continents. In general, $T_e$ is low in young and tectonically active regions (Lowry and Smith, 1994). The rheology and the geothermal gradient, and hence crustal composition, largely affects $T_e$ values. In the ocean, where the composition and thermal evolution of the lithosphere are relatively simple (single layer rheology), the $T_e$ of the lithosphere increases with age and estimates far from active plate boundaries shows values that approximately correspond to the depth of the 450°C isotherm (Watts, 1978).

If the lithosphere behaves like a flexible plate, then the plate structure could be reflected in the seismicity data. This is because seismicity is the consequence of frictional instabilities on sliding surfaces such as faults. Thus, some relationship might exist between the thickness of the depth interval over which earthquakes occur, i.e., seismogenic thickness ($T_s$) and the thickness of the layer that behaves elastically on the long time-scale, $T_e$. Hence, $T_e$ and $T_s$ reflect the strength of the lithosphere. However, Watts and Burov (2003) reveal the fundamental difference in their meanings. They point out that $T_s$ reflects the strength of the uppermost brittle layer of the lithosphere while $T_e$ is indicative of the brittle and ductile strength of the elastic layer. We have better techniques of $T_e$ estimation presently and we need the best estimation of $T_s$, for the detailed relocation of earthquakes, etc., to compare $T_e$ and $T_s$. The similarity between $T_e$ and $T_s$ are much more profound in the oceanic lithosphere than in the continental one

(Weins and Stein, 1984). Several studies (McNutt and Menard, 1982; Burov and Diament, 1992) reveal that $T_e$ decreases with increasing curvature and hence bending stress, while Ts simply reflects the yield stress envelop (YSE) that accounts for the stress generated in a flexed plate by bending. The single layer rheology of the oceanic lithosphere favors the brittle-ductile transition (BDT) within the strong elastic portion (Figure 1.2), and hence correlations can be made between $T_e$ and $T_s$ (Watts and Burov, 2003). The studies on the several deep-sea trench-outer rise systems in the pacific and the Indian Ocean reveal that $T_e$ and $T_s$ are similar for the ages of oceanic lithosphere ≤ 100 Ma (Watts and Burov, 2003). The oceanic lithosphere at the trench-outer rise systems, experiences high curvature because of yielding, and hence $T_e$ is less than it would be. Judge and McNutt (1991), for example, obtained a low Te (22±2 km) in the high-curvature region, which is less than the expected Te (34 km) on the basis of the thermal age of the subducting lithosphere at the northern Chile Trench.

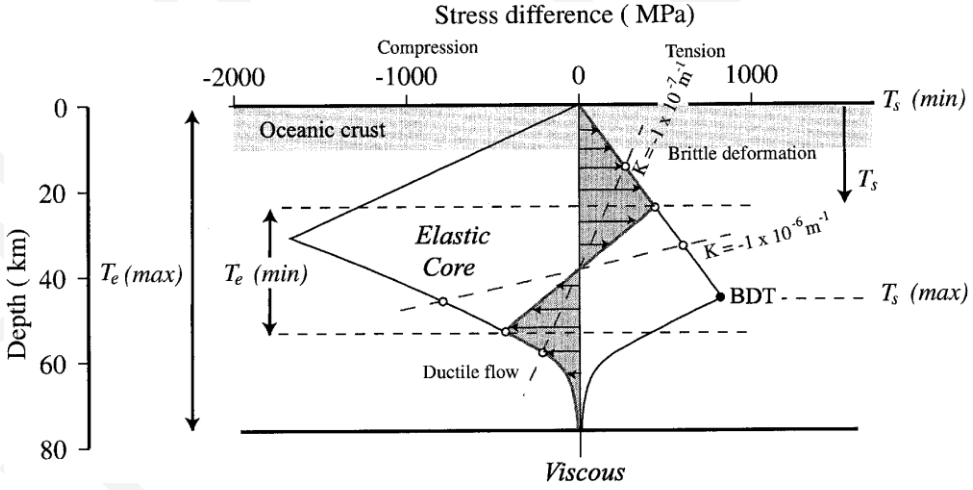


**Figure 1.2:** The Relationship between $T_e$ and $T_s$ for an Idealized Case of Flexure of the Oceanic Lithosphere (After Watts and Burov, 2003). The Thin Solid Line Represents the YSE and the Thick Solid Line Shows the Stress Difference for a Load.

The flexural rigidity of lithosphere can be estimated by direct modeling of the plate response to loading when the load is well known (Watts, 1978). Analysis of the

correlation between the topography and the gravity data, either free air or Bouguer anomaly, using spectral methods provides an alternative to direct modeling. The free air anomaly is a signal corrected for gravity effects caused by the elevation difference between the stations where measurements are taken and sea level. The Bouguer anomaly is further corrected for topographic effects.

## 1.3 Literature Review

### 1.3.1 Measurements in $T_e$ Analysis

Lewis and Dorman made the first attempt to study the isostatic compensation mechanism from the spectral properties of gravity field and topography. They (Lewis and Dorman, 1970) assumed a linear transfer function between Bouguer gravity and topography, the admittance, can be used to describe the mechanism of isostatic compensation. They inverted the admittance to estimate the flexural rigidity of the lithosphere. The admittance Z(k) is computed by taking the ratio of the cross spectra of the gravity and topography to the power spectra in the wavenumber (**k**) domain:

$$Z(k) = \frac{|\langle B(\mathbf{k})H(\mathbf{k})^*\rangle|}{\langle H(\mathbf{k})H(\mathbf{k})^*\rangle} \quad (1.2)$$

where B(**k**) and H(**k**) are the Fourier transforms of gravity and topography respectively.

Some estimates of the elastic thickness of the continental lithosphere based on the admittance were surprisingly low, suggesting that even cratons have no mechanical strength (McNutt and Parker, 1978). These results were later questioned by Forsyth, who showed that the elastic thickness estimated by the admittance method yields too low $T_e$ values if internal loads are not taken into account. He suggested that the coherence between Bouguer gravity and topography yields better estimates of $T_e$ than the admittance, because it allows distinguishing between internal and external loads and is

more sensitive to the elastic thickness than to the loading structure (Forsyth, 1985). One of the main problems with the free-air admittance is related to its higher sensitivity to short-wavelength noise and unaccounted near-surface density variations. Bouguer-based methods are less sensitive to data resolution, and thus, the present study prefers the coherence and admittance methods using Bouguer gravity to compute $T_e$. Figure 1.3 shows the basis of coherence techniques for infinitely strong and infinitely weak plates. However, the actual scenario is intermediate between these two cases. The coherence function ($\gamma$) between gravity and topography field is estimated as:

$$\gamma^2 = \frac{\langle B(\mathbf{k})H(\mathbf{k})^* \rangle^2}{\langle H(\mathbf{k})H(\mathbf{k})^* \rangle \langle B(\mathbf{k})B(\mathbf{k})^* \rangle} \tag{1.3}$$

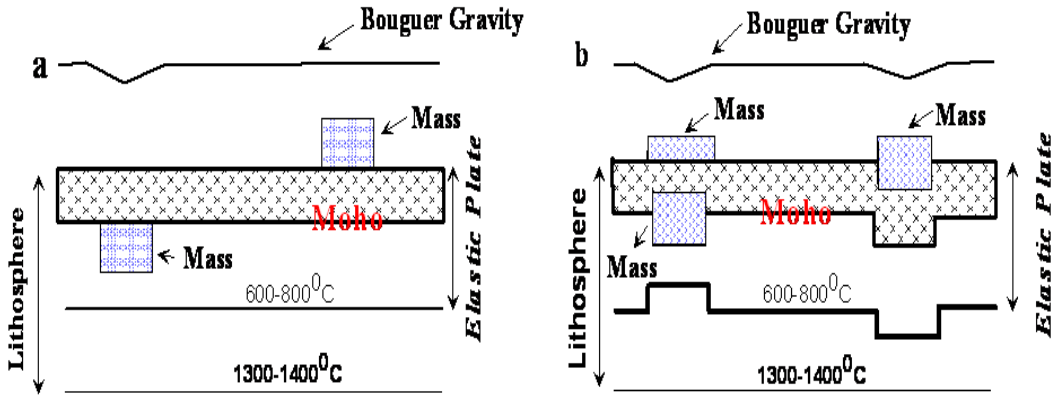


**Figure 1.3:** Basis for Coherence Technique, (a) Infinitely Strong Plate (b) Infinitely Weak Plate.

The estimated values of effective elastic thickness from mirrored periodogram methods and modified periodograms using a single window are found to be less stable than Multitaper methods. This problem was overcome by the Thomson Multitaper method (Thomson, 1982) that extended to two-dimensional fields. The average of several periodograms calculated on data windowed with different Slepian windows proves a good estimator of the coherence and its anisotropy for lithospheric loading problems (Simons et al., 2000). An even better technique to capture the anisotropy of the

continental shield is to use the Hermite Multitaper method as demonstrated by Simons et al. (2003) in the Australian shield. In the past, the spatial variations of $T_e$ have been achieved either by working on a series of adjacent profiles (Stewart and Watts, 1997; Calmant, 1987), or on a mosaic of rectangular areas (Lowry and Smith, 1994; Calmant et al., 1990). The approach was to fit one constant $T_e$ value for a particular area or profile. The modeling of flexure is accomplished either in the spectral domain or in the spatial domain. The data used for such calculations are generally the gravity field and the load due to both the topography or bathymetry, and the crustal density inhomogeneities. However, the spectral method has certain limitations; for instance, the estimated values have poor stability in case of a small topographic load. Moreover, the spectral analysis in 2D requires a square map of topography and gravity data availability, which is not always available due to geographical reasons. Later Kirby and Swain (2004) developed a fan wavelet based method to estimate $T_e$ values. The technique used a superposition of two dimensional Morelet wavelets in a geometry named fan-wavelet, which yield isotropic wavelet coefficients for the co- and cross-spectra of gravity and topography data. They used this technique to compute spatially varying isostatic coherence, and obtained a model fit between the estimated global coherence and the theoretical prediction as well as Fourier transform based estimates. Thus Kirby and Swain (2004) estimated spatially varying $T_e$, for a plate of non-uniform plate thickness. This method has been pretty successful in deriving the $T_e$ structure in continental areas, for e.g., in the Australian shield (Swain and Kirby, 2006), Canadian shield (Audet and Mareschal, 2004) and South American shield (Tassara et al., 2007).

Wavelet methods are used for the univariate time-scale characterization and representation of geophysical fields (Bergeron et al., 2000; Torrence et al., 1998; Rajesh et al., 2004), including their anisotropy (Kumar, 1995). However, the calculation of multivariate coherence functions by wavelet transforms is hampered by lack of suitable

smoothing. A handful of multi-wavelet methods do yield better multivariate time and frequency resolution, but these techniques are restricted to 1-D signals (time series). Simons et al. (1997) formulated a spherical-wavelet-based spatial localization of the admittance between gravity and topography.

To obtain the flexure of a load in spatial domain, initially, the expression of the deformation of the elastic plate due to a point load is determined. The flexure due to an arbitrarily shaped distributed load can then be calculated from the convolution of the point load response function with the load. This procedure was followed by Watts et al. (1975), who obtained the radial response function from a series expansion around the origin of the deflection due to a point load centered at the origin. The method has been used by Cazenave et al. (1980) in oceanic areas (e.g., Calmant, 1987; Calmant et al., 1990). The methodology involves the convolution of the load with the response functions of the elastic plate model to a point load, obtaining the model flexure. The model flexure is compared to the observed flexure of the lithosphere, which is assumed to be equal to the undulations of the CMI (Crust-Mantle-Interface) obtained by constrained gravity inversion or forward modeling. For different values of $T_e$ the flexure is calculated and matched with the modeled gravity field, until a satisfying agreement between the calculated and observed gravity is obtained.

Braitenberg et al. (2002) developed a new approach based on the above mentioned methodology (Watts et al., 1975) to estimate the flexural rigidity of an elastic plate. In this methodology the model flexure is achieved by performing the convolution of the load with the flexural response function of the elastic plate model due to a point load. Figure 1.4 shows the response of flexure due to a point load relative to the flexural rigidity of the lithospheric plate. It shows the resolution limit for calculating the flexural rigidity. The convolution method is advantageous in the sense that the flexural rigidity

can be analyzed over small windows (e.g., 90 km × 90 km). However, for smaller windows sizes, the error increases and the flexural rigidity being a regional parameter, the analysis becomes unreasonable.

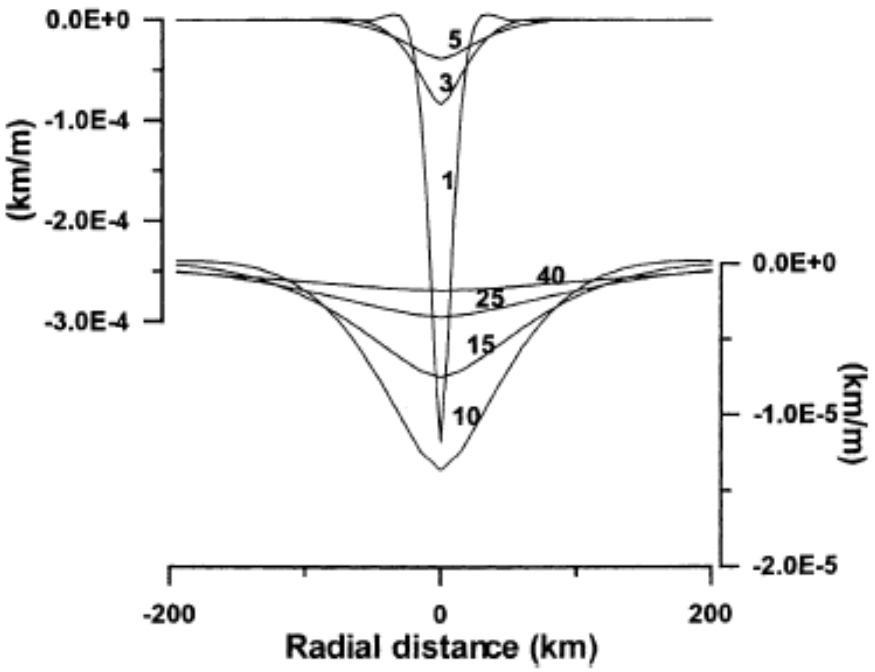


**Figure 1.4:** Flexural Response due to a Point Load for Different $T_e$ Values (Braitenberg et al., 2002). Vertical Axis in the Right Corresponds to $T_e$=1, 3, 5 km and Left Corresponds to $T_e$ =10, 15, 25 and 40 km.

### 1.3.2 Applications of $T_e$

$T_e$ values of 4 km (Cochran, 1979) and 10 km has been estimated in the East Pacific high and Mid-Atlantic ridge respectively using admittance and mirrored periodogram method. Madsen et al. (1984) in the East Pacific Rise (~ 0.7 km) have observed further, lower $T_e$ values. The variations in the method of $T_e$ thus have shown varying relationships between elastic thickness and seismogenic thickness. Kalnins and Watts (2009) used free-air admittance technique to determine the spatial variation of $T_e$ in the western Pacific Ocean. They got a wide range of $T_e$ (0 – 50 km), in which a high $T_e$

obtained over the Hawaiian-Emperor seamount chain, intermediate values over the Marshall Islands, Gilbert Ridge, and Marcus-Wake Guyots and a low $T_e$ range over Line Islands, Mid-Pacific Mountains, Caroline Islands, Shatsky Rise, Hess Rise, and Musician Seamounts. They obtained a pattern of low $T_e$ over oceanic plateaux in the study region, including the Ontong-Java Plateau and the Manihiki Plateau. They suggested this uniform $T_e$ seen low over the oceanic plateau may reflect their formation at a spreading centre. Watts and Ten Brink (1989) explained the high $T_e$ range obtained over the Hawaiian Ridge as being the result of the unbending of the lithosphere due to magmatic underplating. They concluded that the negatively buoyant underplating is coherent with the surface volcanic load, but has a longer wavelength.

Daly et al. (2004) compared multitaper and wavelets methods to analyze the coherence between Bouguer gravity and bathymetry data over the Irish Atlantic margin, and obtained low $T_e$ values (6–8 km). They found the weakest lithosphere in the Southern Rockall basin, Porcupine bank and Porcupine basin and the strongest lithosphere along the Rockall-Hatton region. They concluded that the low $T_e$ was frozen into the lithosphere at the time of emplacement of loads during the continental breakup. Further, they considered the process of sedimentation and the presence of fluids as contributory factors for the low $T_e$ estimates. Earlier studies done by Chand et al. (2001) used 1D profile for free-air admittance method to establish the possible mechanism of rifting and shearing occurring in the conjugate margin of eastern continental margin of India and Eastern Antarctica continental margin. They obtained a clear demarcation of rifting and shearing in these conjugate margins based on spatial $T_e$ variations. They obtained a relatively low elastic thickness around 5 km in the southern part to about 10–25 km towards the northern part of the eastern margin of India. Chand et al. (2001) interpreted the high $T_e$ of 10–25 km as evidence for sheared character of the margin.

Perez-Gussinye et al. (2008) used 2D Multitaper coherence of Bouguer gravity and topography data along the Andean margin to estimate $T_e$ by using the Forsyth model (1985). In order to estimate $T_e$, they compared observed coherence with curves predicted for a range of $T_e$ values, and calculated the surface and sub-surface loads and compensating deflections that exactly reproduce the observed topography and gravity anomaly. In the next step, they calculated a predicted coherence by assuming that surface and sub-surface loads are statistically uncorrelated. Finally, the $T_e$ value that minimizes the difference between predicted and observed coherence is assigned as the $T_e$ for the analyzed area. They obtained $T_e$ variations that is highest (~ 40 km) in the fore-arc (~ 20°S) and interpreted this $T_e$ structure due to conductive cooling of the continent by the subducting slab. In addition, a low $T_e$ of 20 km in the Central Andes along the volcanic chain and Altiplano plateaus is interpreted as being due to high geothermal gradient. Perez-Gussinye et al. (2008) used large window sizes 600×600 $km^2$ and their further analysis and tests revealed that the window size could retrieve $T_e$ values up to 60 km. These results are consistent with the $T_e$ ranges obtained by the 2D forward modeling of Tassara (2005). He tested the spatial variation of fore-arc rigidity and along strike gradients of horizontal stresses and obtained a high rigidity ($T_e$ > 50 km) in the fore-arc region which decreases sharply toward the weak main orogen ($T_e$ < 10 km). Tassara (2005) concluded that north-south weakening of the fore-arc could be mainly due to the decreasing thermal age of the Nazca slab below the continent and can be also correlated to the increased frictional heating driven by the southward flattening of the subducted slab.

In another study, Tassara et al. (2007), using a land-ocean scheme in South-American plate, suggested the use of Banks model (Banks et al., 2001) instead of the Forsyth model to avoid numerical instabilities if the anomalies have shallow sources in a subduction scenario. Their analysis could reveal the rigidity structure which followed the

segmentation of the seismogenic zone along the subduction fault. Kudo et al. (2001) used Bouguer coherence to estimate the effective elastic thickness of the Japanese Island arc, and obtained various $T_e$ from 3 km to > 20 km. Their $T_e$ results showed a good correlation with the heat flow, and that the plate was elastically thin where the heat flow is high. They attributed smaller $T_e$ obtained over the Northern Ryukyu arc to the extensional tectonics in that region, but treated the subduction of a shallow slab beneath the south-western Japan frontal arc as a possible reason for the increasing $T_e$ estimates. Billen and Gurnis (2005), using the admittance technique, obtained a decrease in the effective elastic thickness by at least 15 km as approaching the Kermadec trench within the Pacific Ocean plate. Their results suggest that significant dissipation of energy occurs within less than 100 km of the trench axis, and this has been attributed to the occurrence of large-scale normal faulting events in the subducting plate which is responsible for the elastic strength reduction.

The first attempts to estimate $T_e$ in the Indian craton was made by Karner and Watts (1983) and also by Lyon-Caen and Molnar (1985). Using forward modeling between Bouguer anomaly and topography they obtained $T_e$ values of 80 to110 km in the Ganges basin. Free air admittance by McKenzie and Fairhead (1997) yielded low $T_e$ values of 24 km which is found to be correlated with seismogenic thickness ($T_s$). However, subsequent studies by Handy and Brun (2003) suggested that $T_e$ can very well exceed $T_s$ as well. Rajesh and Mishra (2003) using Multitaper spectral analysis characterized the relative variation of $T_e$ in the India – Eurasia collision zones. In another analysis, Rajesh and Mishra (2004) used the transitional coherence wavelength in characterizing the tectonic provinces. Jordan and Watts (2005) used both forward and inverse flexural and gravity modeling techniques and obtained a spatially varying $T_e$ structure ranging from 0 to 125 km in the India – Eurasia collision zones.

Tiwari et al. (2003) conducted studies using spectral admittance in the Ninety East Ridge adjacent to the Indonesian continental margin. They obtained comparatively high $T_e$ values over the northern ($T_e$ ~ 17 km) and Southern ($T_e$ ~ 22 km) parts of the NER. However, in the central blocks the results showed zero strength ($T_e$ ~ 0 km). Their assumption was that the high $T_e$ regions have emplaced on relatively older lithosphere through an off-ridge intraplate volcanism. They have also suggested that the southern part was emplaced over the Antarctic/Australian plate along the fracture zone. The low $T_e$ values over the central blocks led them to infer that the thick underplated crust in the central part might have resulted from the interaction of the hot spot with the extinct Wharton spreading ridge.

### 1.4 Scope of the Present Work

The present study uses Bouguer coherence and Bouguer admittance methodology in convergent (Indonesian active margin) and divergent margins (North America passive margin) and compares the results with respect to earlier methods. McKenzie (1997, 2003) has pointed out that in regions of low topography, large elastic thickness may be due to the unmodeled presence of buried loads. McKenzie advocated free-air gravity anomaly rather than the Bouguer gravity anomaly, and the admittance rather than the coherence between gravity and topography. At long wavelengths, the Bouguer anomaly is coherent with the topography as the surface (or internal) loads are fully compensated. Hence the present estimation ensures that the coherence or admittance method using Bouguer gravity anomaly should lead to results that are quantitatively interpretable on the level. Both methods use information about the Earth's gravity and topography, and both form different ratios of their spectral energy density. Studies argue that the difference in absolute value of the effective elastic thickness between competing analysis methods is significant for the proper accounting of the statistics of the estimates. Several studies

confirm that relative variation of elastic thickness with its corresponding statistics is significant with respect to the respective tectonic domains. We consider it beyond the scope of this work.

In principle, though, if the coherence is generally low, the Forsyth's model is not going to be valid, and any coherence-based modeling is bound to fail. More-over, if we have two independent loading processes on two different interfaces, then we cannot really work with the coherence at all. In such cases, the present study recommends that the use of Bouguer admittance will provide much more insight into the degree to which the region is flexurally compensated. It is nearly impossible to interpret a particular value of the coherence as "significant" without looking in detail at the statistics. So the statistics including the loading ratio and error indicates that Bouguer admittance is valuable for constraining the spatial extend and magnitude of variation in elastic strength in convergent as well as divergent margins. Above all, the study based on the $T_e$ estimates obtained from the same analytical tools on the two continental margins of entirely opposite nature would be an interesting and timely way to understand the diversity in their geodynamic setting.

### 1.5 Aim of the Study

The present study focuses on the estimation of effective elastic thickness on an active (convergent) as well as passive (divergent) plate margin using the multi-taper based Bouguer coherence and wavelet based Bouguer admittance methodologies. The main aim is to characterize the tectonic behavior of the different zones of these margins, and thereby segmentize them by correlating the $T_e$ estimates with other tectonic parameters such as lithospheric age, heat flow, seismicity, major morphologic features, sedimentation, fault structures, depth of necking and so on.

## 1.6 Objectives

The present research work focuses on the reappraisal of the variation of effective elastic thickness in the active and passive margins. In view of this, the objectives of the study are as follows:

**(i)** To assess the mechanical strength along the Indonesian active continental margin by applying the multi-taper technique. The study reveals a correlation of the variation of mechanical strength to the sediment load, prevailing heat flow and the shear wave anomaly.

**(ii)** To estimate the spatial variation of effective elastic thickness along the Andaman-Sumatra-Java subduction zone in the eastern Indian Ocean. The more appropriate Banks model (Banks et al., 1977) has been followed in the analysis. The study uses Bouguer admittance estimates to examine whether rigidity structure in the study area has any causal relationship with the segmentation of the seismogenic zone.

**(iii)** To recover the mechanical strength of the north east passive margin of North America by using multitaper techniques. The aim is to investigate the isostatic elastic thickness and transitional wavelength for the region in six zones using improved orthonormalized Hermite multi-tapers derived Bouguer coherence.

**(iv)** To estimate spatial $T_e$ variation over the North American passive margin by using Bouguer Admittance technique. The aim of the study is to understand the long-term strength variation along of the margin and to locate the ocean-continent transitional zone.

## 1.7 Study Regions

The present study is the analysis of two entirely different plate margins of this globe, such as the convergent and the passive divergent continental margins. A

convergent margin can be defined as the leading edge of the continent where subduction takes place. These margins are the regions of immense tectonic activities, including earthquakes, volcanoes, mountain building, etc. In contrast, a divergent margin is the transition zone from continental lithosphere to oceanic lithosphere where there is no collision or subduction takes place. These margins originally formed during continental rifting and are of two types: volcanic and non-volcanic rifted margins. The characteristic processes on divergent margins include active subsidence, sedimentation, growth faulting, pore fluid formation and migration, etc.

A classical example of the subduction system in the Indonesian continental margin (Andaman-Sumatra-Java subduction zone) has been taken for the analysis of a convergent margin. In scrutiny of a divergent margin, the typical non-volcanic rifted margin and adjacent rifted basins of North America (North Atlantic) have been assigned. The description of these study regions are as follows.

### 1.7.1 Indonesian Active Continental Margin:

The Indonesian continental margin (Figure 1.5) is located in the eastern Indian Ocean which forms the boundary between the Indo-Australian plate and the Eurasian plate. It is widely debated that large portions of the Marion, Kerguelen and Reunion hot spots contributed to the heating up of the lithosphere, eventually resulting in the breakup of Gondwanaland about 140 Ma ago. The breakup of Gondwanaland into Africa, Antarctica, Australia and India is thought to have resulted in the opening of the Indian Ocean. (Gaina et al., 2007).The northward movement of the Indian plate attained very high speed (18–20 $cmYr^{-1}$) during the Cretaceous period, and then slowed to ~5 $cmYr^{-1}$ after the collision with the Eurasia about 50 Ma ago (Curray et al., 1982; Klootwijk et al., 1992). Subsequently, the India-Antarctica and the Australia-Antarctica ridges merged together to form a single continuous spreading ridge, the Southeast Indian Ridge. As a

consequence, the Indian plate and the Australian plate became a single Indo-Australian plate.

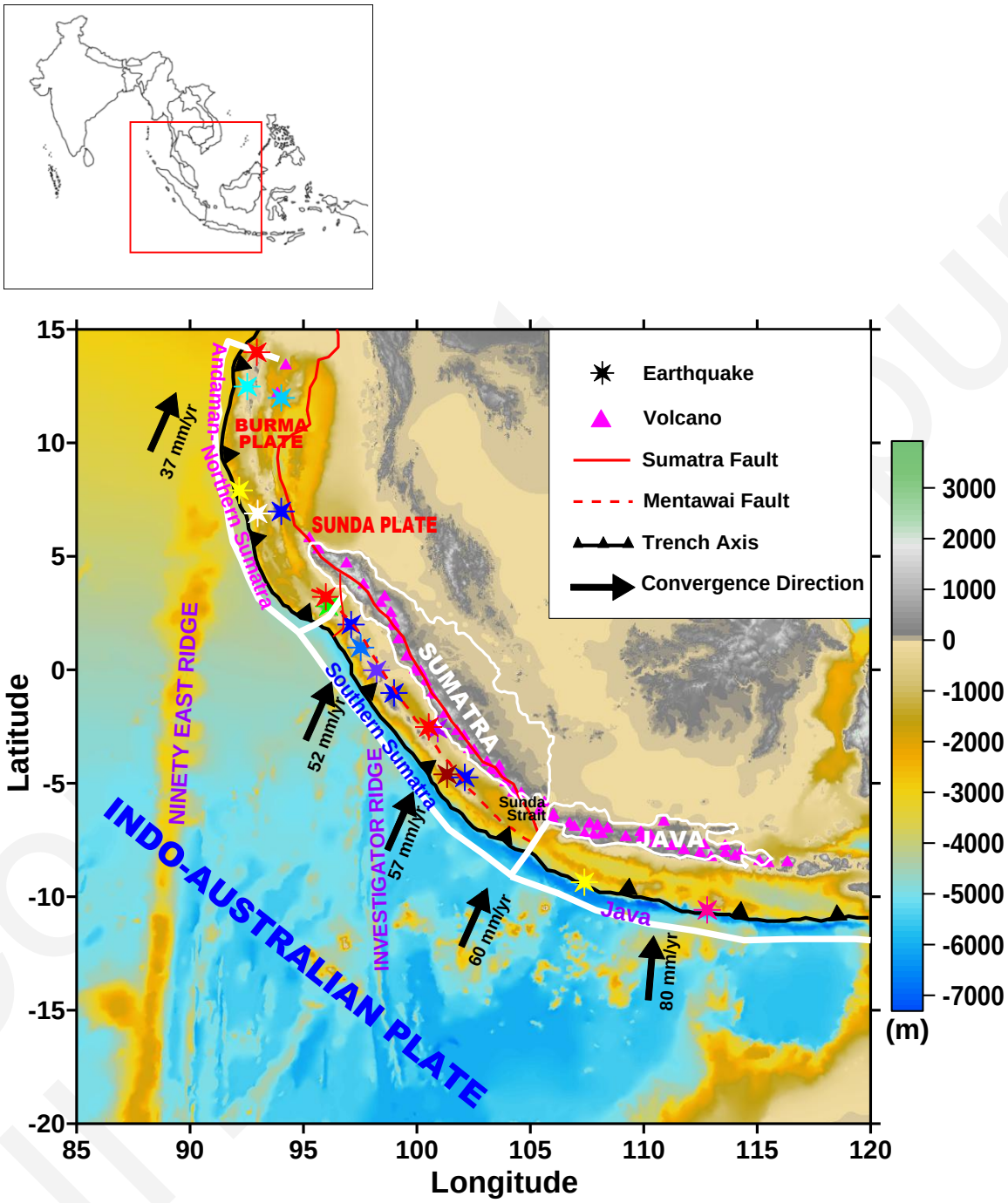


**Figure 1.5:** Inset (top) shows the Location of Study Area with respect to India. Bathymetry Map (Bottom) Exhibits Major Morphological Features of the Indonesian Continental Margin.

During the rapid northward drifting, the Indian plate also rotated in a counter-clockwise direction. Thus the greater Indian continent had collided with the Eurasia obliquely along the plate's eastern boundary (the Burma-Andaman-Malay region). The transform forces along this subduction front started the clockwise bending of the Sunda arc (Curray, 2005). In the late Oligocene, further faulting developed and the Burma and Sunda microplates began to "break off" from the larger Eurasian plate. In the early Miocene, backarc spreading started forming the sea floor which later became the Alcock and Sewell Rises.

From middle Miocene, these contiguous features were separated from the foot of the continental slope by NW-SE spreading, and the motion of the southern part of the West Andaman Fault was taken up by the Mentawai Fault in the fore-arc basin off Sumatra. At about 3–4 Ma, the present plate edge was formed, Alcock and Sewell were separated by formation of the central Andaman Basin, and the faulting started moving from the Mentawai Fault to the Sumatra Fault System bisecting Sumatra.

The Indonesian continental boundary (Figure 1.5) is a prototype complex subduction system, composed of the down going Indo-Australian slab beneath the Sunda and Burma tectonic plates along the Andaman-Sumatra-Java subduction zones from north to south respectively (Curray et al., 1979; Kamesh Raju et al., 2007; Curray, 2005). The major features formed due to this process are an accretionary wedge, the outer arc forming the backstop and fore-arc basins (Samuel et al., 1997; Schluter et al., 2002). Two strike slip fault components are traverse through the Sumatra margin, known as the Sumatra and Mentawai fault segments (Malod, 1995). The Sumatran Fault Zone (SFZ) accommodates most of the strike slip motion associated with the oblique convergence between the Indo-Australian and Burma-Sunda plates.

The prominent structures on the subducting Indo-Australian plates adjacent to the subduction zone are the aseismic ridge segments such as the Ninety-east Ridge (NER), Investigator Ridge, etc. Indian Ocean subduction zone is one of the most active plate margins of the globe, as evident from its vast record of great magnitude earthquake and tsunami events. The great Sumatra-Andaman earthquake and tsunami of 2004 was a dramatic reminder that the convergent margins are potentially active, destructively dangerous and totally unpredictable places on the Earth. Hence, detailed and comprehensive analyses are essential to understand the seismic processes in subduction zones.

### 1.7.2 North East Passive Margin of North America

North east passive margins of North America (Figure 1.6) represents the rifting of the super continent Pangea about 200 million years ago, first as North America separated from Africa and then as it separated from Europe and England. The rifting thinned and heated the continental crust and lithosphere, which then subsided to form a complex set of marginal basins. The North Atlantic passive continental margins are unique due to their undisturbed tectonic quiescence dominated by lithospheric cooling subsequent to continental break up (Mckenzie, 1978; White, 2003). The rifting along the northernmost portion of this margin, especially in the offshore of Nova Scotia and Newfoundland is remarkably magma poor. However, the southern segment that includes the southeastern United States was associated with voluminous magmatism. The sedimentary prism in many of this margin basins show large differences in synrift and post-rift evolution (Keen, 1989). The different geometries and structures evidenced from the comparison of the conjugate margins suggest the asymmetry in the lithospheric extension and margin development during rifting (Lister et al., 1986).

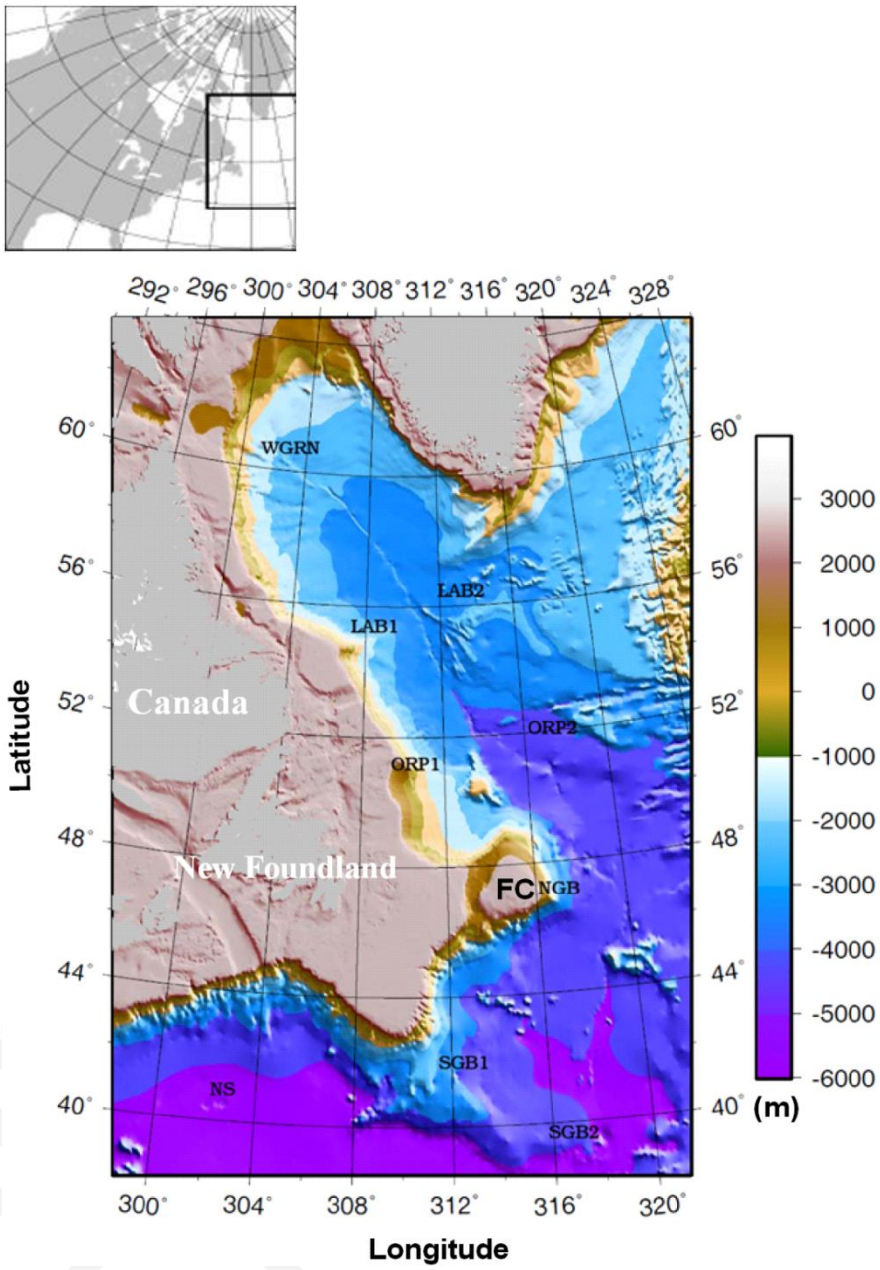


**Figure 1.6**: Inset (top) shows the Location of Study Area with respect to North America. Bathymetry Map (Bottom) Exhibits Locations of Six Transects Assigned for the Study, Include West Greenland (WGRN), Labrador (LAB), Orphan Basin (ORP), Northern Grand Bank (NGB) and Flemish Cap (FC), Southern Grand Banks (SGB), and Nova Scotia (NS).

The Northeast Atlantic margin is an ideal setting to study the crustal responses under large amounts of extension in the northeastern rifted margins, since it is characterized by lack of significant volcanism during the late stages of rifting and

continental break-up, and relatively thin sediment sequences deposited over the continental slope, rise, and abyssal plains. The present study covers the six transects (Figure 1.6) in the north east margin of North America, namely, West Greenland (WGRN), Labrador (LAB), Orphan Basin (ORP), Northern Grand Bank (NGB), Southern Grand Banks (SGB), and Nova Scotia (NS).